Inhibiting Polyamide Intrusion of Thin Film Composite Membranes: Strategies and Environmental Implications

Yukun Qian[a], Haozheng Li[a], Jiancong Lu[b], Dan Lu[a], Hongyu Jin[a], Zhiyi Xia[a], Zhikan Yao[a, d, *], Jing Wang[a, e], Lin Zhang[a, c, e], Chuyang Y. Tang[f]

a. MOE Engineering Research Center of Membrane and Water Treatment Technology, College of Chemical and Biological Engineering, Zhejiang University, Hangzhou, 310027, P. R. China

b. Ocean College, Zhejiang University, Zhoushan, 316021, P. R. China

c. Institute of Zhejiang University-Quzhou, Quzhou, 324000, P. R. China

d. Shanxi-Zheda Institute of Advanced Materials and Chemical Engineering, Taiyuan, 030000, P.R. China

e. Ningbo Research Institute, Zhejiang University, Ningbo, 315100, P. R. China

f. Department of Civil Engineering, The University of Hong Kong, Pokfulam, Hong Kong Special Administrative Region, 999077, P. R. China

*Corresponding author.

E-mail address: yaozhikan@zju.edu.cn (Zhikan Yao)

Abstract

Thin film composite polyamide (TFC) nanofiltration (NF) membranes represent extensive applications at the water-energy-environment nexus, which motivates unremitting efforts to explore membranes with higher performance. Intrusion of polyamide into substrate pores greatly restricts the overall membrane permeance because of the excessive hydraulic resistance, while the effective inhibition of intrusion remains technically challenging. Herein, we propose a synergetic regulation strategy of pore size and surface chemical composition of the substrate to optimize selective layer structure, achieving the inhibition of polyamide intrusion effective for the membrane separation performance enhancement. Although reducing the pore size of the substrate prevented polyamide intrusion at the intrapore, the membrane permeance was adversely affected due to the exacerbated “funnel effect”. Optimizing the polyamide structure via surface chemical modification of the substrate, where reactive amino sites were in-suit introduced by the ammonolysis of polyethersulfone substrate, allowed for maximum membrane permeance without reducing the substrate pore size. The optimal membrane exhibited excellent water permeance, ion selectivity, and emerging contaminants removal capability. The accurate optimization of selective layer is anticipated to provide a new avenue for the state-of-the-art membrane fabrication, which opens opportunities for promoting more efficient membrane-based water treatment applications.

Keywords: nanofiltration membranes; substrates; interfacial polymerization; polyamide intrusion; emerging contaminants; water treatment

Synopsis: NF membrane prepared with polyamide intrusion inhibition strategy reduces hydraulic resistance and optimizes polyamide structure, achieving enhanced membrane separation performance and emerging contaminants removal.

1. Introduction

Thin film composite (TFC) nanofiltration (NF) membranes play a vital role in the water-energy-environment nexus, including water treatment and high-value resource recovery,[1-4] because of its excellent solute-water and solute-solute selectivity.[5] The fabrication of high-performance TFC membranes is the key to improve the processing efficiency for target species.[6] In general, high-performance membranes should possess features of thin selective layer thickness for low hydraulic resistance, high cross-linking and narrow pore size distribution for precise solute selectivity.[7-9] Polyamide selective layers are typically prepared on porous substrates by the water/oil interfacial polymerization (IP), in which the IP process is considered to be governed by reaction-diffusion kinetics.[10, 11] The properties of the selective layer are affected by many factors, such as monomers, additives, substrate and reaction temperature.[12-14] In particular, substrate, as the forming interface and support of the polyamide layer, performed a profound impact on the selective layer structure and membrane performance.[15-17]

Improving substrate properties, such as constructing the interlayers and optimizing the surface structure of substrates, could effectively enhance membrane permeance. A common belief is that the improved membrane performance by substrate modification is ascribed to the role of substrates in altering monomer diffusion, leading to the variations in crosslinking or thickness of polyamide framework. Nevertheless, subtle changes at the selective layer−substrate interface, where the polyamide layer adheres to the substrate surface, are often overlooked during the IP process.

Previous studies reported the phenomenon of polyamide intrusion at the selective layer-substrate interface,[18-20] which ensured the stable operation of membranes during the cross-flow separation process. This unintentional intrusion is commonly caused by an irregular reaction interface during the IP process, where the aqueous meniscus might drop below the substrate interface, resulting in a deeper formation of the polyamide within the substrate pores.[18, 21] Recent studies have confirmed that various properties of TFC membranes such as water permeance and mechanical stability are closely associated with polyamide intrusion.[16, 20] Appropriate penetration of polyamide into the substrate could promote the mechanical stability of the membrane by forming

anchorages within the substrate.[20, 22] However, excessive polyamide intrusion inevitably increases the transport distance and resistance, which is detrimental to the separation performance of TFC membranes.[23-25] Moreover, this adverse effect will be further amplified since all the water has to transport through this intrusion, whose available area is limited by the surface porosity of the substrate.[23] Therefore, the systematic control of polyamide intrusion is of great significance. Up to date, the underlying mechanisms of polyamide intrusion are not exactly understood, and effective ways of intrusion inhibition are yet to be paved.

In this study, we propose an effective strategy based on the synergistic regulation of the pore size and surface chemical composition of the substrate to inhibit polyamide intrusion. The mechanism of the generation of polyamide intrusion was further revealed via the investigation of the substrates with variable pore sizes. In particular, enhanced water permeance and emerging contaminant removal were observed for NF membranes prepared with the novel strategy. Our study provides a new avenue for the fabrication of high-performance TFC membranes, which opens opportunities for promoting highly efficient membrane-based water treatment applications.

2. Experimental section

2.1 Materials

Commercial polyether sulfone (PES) ultrafiltration membranes with different molecular weight cutoff (MWCO) were purchased from the Microdynes-Nadir company as substrates, and named PES-s (5 KDa), PES-m (20 KDa), and PES-l (150 KDa) in sequence according to the pore size from small to large. Diethylenetriamine (DETA, 99%, Macklin) was utilized as the surface amination reactant to prepare the surface aminated substrate. Analytical reagents including Na_2SO_4, NaCl, Na_3PO_4, NaOH, HCl, N,N-Dimethylformamide (DMF), ethanol, and n-Hexane (97%) were all procured from Macklin Reagent Co., Ltd. (Shanghai, China). Piperazine (PIP, 99%, Macklin Inc.) and trimesoyl chloride (TMC, 99%, J&K Scientific Ltd.) were used as the monomers for IP reaction. Deionized water used in this study was obtained from a laboratory-made system.

2.2 Preparation of surface aminated substrates

The surface amination of the PES substrate was carried out following our previous

work.[24] Briefly, the completely washed PES membranes were immersed into a 10 wt% DETA aqueous solution to perform the aminolysis reaction. After reacting at 90 ℃ for several hours, the surface aminated PES substrates were thoroughly washed by ethanol and deionized water successively. Finally, the substrates were stored in deionized water before use. It should be noted that the surface amino content of the substrates was controlled to a comparable amount by adjusting the amination reaction time (Figure S1). The original substrates with different pore sizes were named as PES-n-O, where n referred to the pore sizes of substrates. Correspondingly, the surface aminated substrates were named as PES-n-A.

2.3 Preparation of TFC polyamide membranes

TFC membranes were prepared by a typical IP reaction. The PES substrates were first soaked in the PIP aqueous solution (0.5 w/v%) for 2 min. The excess solution was thoroughly removed by a rubber roller. Then, the substrates were immersed in the TMC n-hexane solution (0.05 w/v%) for 1 min to form the polyamide selective layers. Subsequently, a thermal treatment (50 °C, 10 min) for the membranes was performed. The obtained TFC membranes were named TFC-n-O, or TFC-n-A based on the substrate used for the membrane preparation.

2.4 Characterizations of membranes

The morphologies of the membranes were characterized by scanning electron microscopy (SEM, SU-8010, Hitachi) following similar procedures to the previous study.[26] The thickness and surface roughness of membranes were measured by atomic force microscopy (AFM, Dimension Icon, Bruker) on silicon wafers with a scanning range of 5 μm × 5 μm. High resolution images of TFC membranes were obtained by transmission electron microscope (TEM, JEM-2100F, JEOL). The TFC membrane was firstly embedded in a resin and then cut into 80 nm slices. The rear side of the selective layer was sampled by similar procedures referring to the previous study by using DMF as the solution to fully dissolve the PES substrate.[27] The front side and rear side chemical composition of the selective layer were then explored by X-ray photoelectron spectroscopy (XPS, EscaLab 250Xi, Thermo Scientific).

The surface hydrophilicity of membranes was characterized by a contact angle goniometer (ASE, GBX Scientific). SurPASS electrokinetic analyzer (SurPASS™ 3, Anton Paar) was used to obtain the surface charge properties (zeta-potential) of the TFC membranes.

The pore size and distribution of the membranes were determined by using a solute transport approach based on the association between solute sizes and solute rejection rates.[28] Briefly, the pore size is assumed to have a log-normal distribution following Equation 1:

$$\frac{dR(r_p)}{dr_p} = \frac{1}{r_p ln\sigma_p \sqrt{2\pi}} exp\left[-\frac{(lnr_p - ln\mu_p)^2}{2(ln\sigma_p)^2}\right] \quad (1)$$

where r_p is the Stokes radius of the feed solute, R is the solute rejection, μ_p is the mean pore size, and σ_p is the geometric standard deviation of the probability density function curve. Observed solute rejection rates were calculated by Equation 2:

$$R = \left(1 - \frac{C_p}{C_f}\right) \times 100\% \quad (2)$$

where C_p and C_f (mg/L) are the concentrations of solute in the permeate and feed, respectively. In this study, feed solutions containing 200 ppm of various molecular weights of PEG (10,000 and 20,000 Da) and PEO (100,000 and 300,000 Da) were utilized to evaluate the substrate pore sizes and distributions. The Stock radius of PEG or PEO in the test can be calculated by Equation 3 or Equation 4:

For PEG, $r_s = 16.73 \times 10^{-10} MW^{0.557}$ (3)

For PEO, $r_s = 10.44 \times 10^{-10} MW^{0.587}$ (4)

where r_s (nm) and MW (Da) are the Stokes radius and the average molecular weight of PEG or PEO, respectively. In addition, the pore size and pore size distribution of the TFC membranes were estimated by a series of neutral glycosides with increasing molecular weight, including glycerol (92 Da), glucose (180 Da), sucrose (342 Da), and raffinose (504 Da).[29] The Stokes radius of these carbohydrate molecules correlates with their molecular weight by Equation 5:

$$\ln(r_s) = -1.4962 + 0.4654 \ln(MW) \quad (5)$$

2.5 PIP diffusion tests

The PIP diffusion was tested by observing the diffused PIP from the aqueous phase into the organic phase using a UV-vis spectrophotometer (UV-1900i, SHIMADZU).[30] In detail, 20 mL of aqueous phase solution (0.5 w/v% PIP) was placed on the top of aminated substrates at 25℃ for a 120 s retention time, followed by the same volume of organic phase solvent (n-hexane) being lightly poured upon the aqueous phase solution. After a 60 s diffusion period, 3 mL of PIP-containing n-hexane was gently extracted from the near interface of two phases by a pipette and measured by a UV-vis

spectrophotometer.[31] The relative PIP concentration was determined according to a characteristic absorption peak at 208 nm (Figure S2). The PIP diffusion test of the original substrates was also operated for comparison.

2.6 Membrane separation performance

A lab-made cross-flow membrane filtration device was acquired to evaluate the pure water flux and salt rejection of the manufactured TFC membranes under 5 bar at 25 ± 1 °C. Each TFC membrane was placed in a cross-flow cell (CF016P, Sterlitech) with a filtration area of 20.6 cm^2.[32] The membranes were all pre-compressed at 5 bar for 30 minutes before the test. Aqueous solutions with 2000 ppm inorganic salt (Na_2SO_4, NaCl) were used as feed solutions for selectivity measurements. The water flux (J_v, $L/m^2 \cdot h$), permeance coefficient (A, $L/m^2 \cdot h \cdot bar$),[33] and salt rejection (R, %) of membranes can be determined by Equation 6-8:

$$J_v = \frac{\Delta V}{\Delta t \times a} \tag{6}$$

$$A = \frac{J_v}{\Delta p} \tag{7}$$

where ΔV (L) is the permeated volume of water collected in Δt (h), a (m^2) is the available area of the membrane, and Δp (bar) is the pressure difference across the membrane.

$$R = \frac{C_f - C_p}{C_f} \times 100\% \tag{8}$$

where C_f (mg/L) and C_p (mg/L) are the salt concentration of the feed and permeate, respectively, determined by an electrical conductivity meter (FE30, Mettler).[34] The salt permeability coefficient (B, $g/m^2 \cdot h$) was calculated by Equation 9, based on the classical solution-diffusion theory:[32]

$$B = \frac{(1-R) \times A \times (\Delta p - \Delta \pi)}{R} \tag{9}$$

where $\Delta \pi$ (bar) is the osmotic pressure difference across the membrane. Salt separation factor (α), a parameter to determine the Na_2SO_4 to NaCl selectivity of the TFC membrane,[35] was based on Equation 10:

$$\alpha(Na_2SO_4/NaCl) = \frac{(C_{NaCl}/C_{Na_2SO_4})_p}{(C_{NaCl}/C_{Na_2SO_4})_f} = \frac{1-R_{NaCl}}{1-R_{Na_2SO_4}} \tag{10}$$

In addition, emerging contaminant removal tests were also performed under the same conditions. To simulate the presence of emerging contaminant in the ecosystem, 10 ppm tetracycline was introduced to the feed solution containing 10 mM NaCl.[36] Each

experiment was continued for 2 h. Subsequently, 5 mL of the permeate and feed solution were extracted separately to determine the concentration of tetracycline using high performance liquid chromatography (HPLC, LC-20AT, SHIMADZU). Specifically, the concentration of tetracycline in different solution was obtained by means of the standard curve (Figure S3). The rejection of tetracycline by the prepared TFC membranes was obtained following Equation 8 mentioned above.

3. Results and discussion

3.1 Characterization of the substrates

The surface amino group content of aminated substrates were adjusted to be similar (~0.5 mmol/m^2) by controlling the amination reaction time (Figure S1). Afterwards, the aminated substrates with different pore sizes were compared with the corresponding inert original substrates (0 mmol/m^2). The characterization of these substrates was shown in Figure S4, Figure S5 and Table S1. The slight variations in pore size, porosity, and roughness of aminated substrates were due to the slight degradation during the amination reaction.[37] Figure 1a-c further presents the pore size distribution curves of the original and aminated substrates. The widened pore size distribution of the aminated substrate resulted from its slightly increased effective pore size. In general, the slight change in substrate pore size and pore size distribution caused by the amination reaction was negligible compared to the relatively large pore size of the original substrate itself. Furthermore, the marginally increased hydrophilicity of the aminated substrates could be attributed to the grafting of amino groups on the surface of the substrates (Figure S6). Therefore, the amination reaction successfully introduced amino groups on the surface of the original substrates without causing major changes in its physical structure.

The results of the PIP diffusion experiments indicated that the concentration of PIP in the organic phase tended to be lower for the aminated substrates (Figure 1d). The slower diffusion rate of PIP to the organic side at the interface could be attributed to the amino groups on the aminated substrate that could bind to the PIP by hydrogen bonding interactions.[38] As a result, the amino groups on the substrate surface were expected to have a significant impact on the IP process, potentially facilitating the regulation of membrane structure and performance.

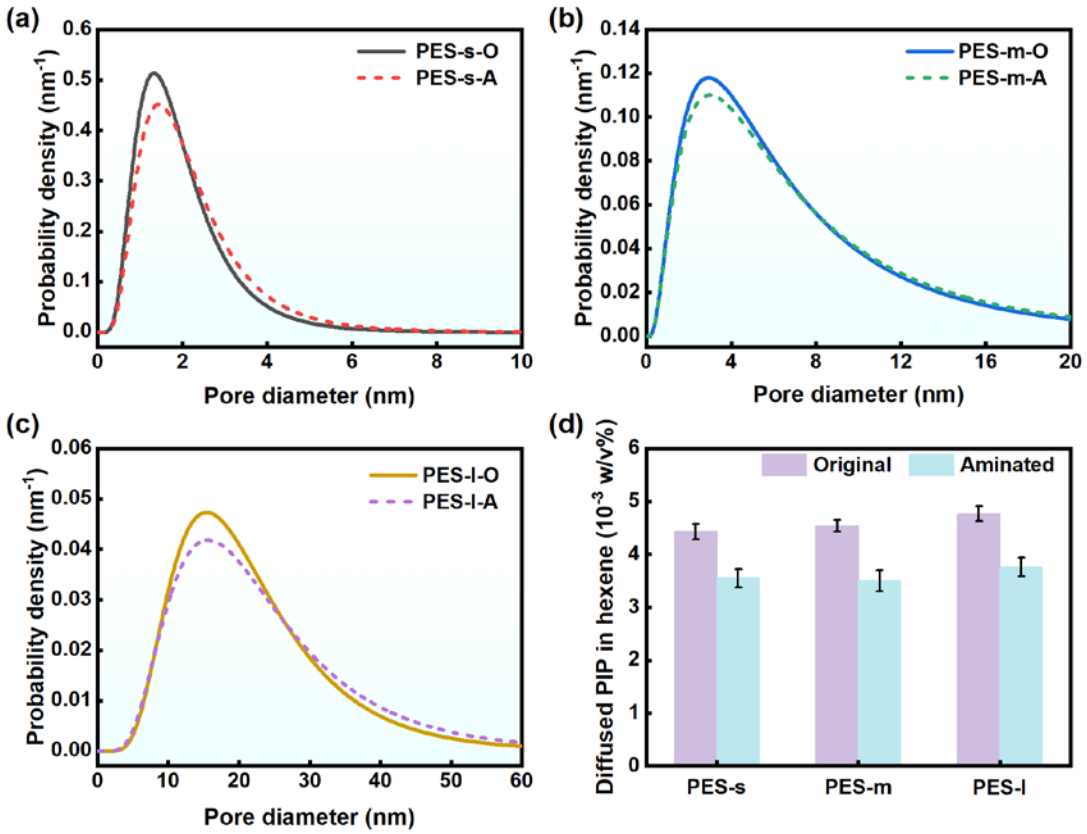

Figure 1. Characterization of the substrates: the pore size distribution of (a) PES-s-O/A, (b) PES-m-O/A, (c) PES-l-O/A; (d) Concentration of PIP diffused into the organic side (hexane) before and after substrates amination.

3.2 Characterization of TFC membranes

Microscopic morphologies of the prepared TFC membranes were evaluated by SEM (Figure 2). All the TFC membranes demonstrated similar nodular-like surface morphologies, which was typical for nanofiltration membranes produced by PIP/TMC IP reaction. According to the results of AFM characterization (Figure S7, Table S2), the surface average roughness of TFC-n-A was slightly reduced compared to the control TFC-n-O. This result indicated that selective layers with more ordered and homogeneous raised structures were formed on the aminated substrates, which could be explained by the hindered diffusion of monomers by the amino groups on the aminated substrates.

In addition, SEM was used for analyzing the rear surfaces of the prepared TFC membranes after dissolving their PES substrates (Figure 2). Distinctive morphologies were observed on the backside of the selective layer of these TFC membranes unexpectedly. The control TFC-n-O series (TFC-m-O and TFC-l-O) show numerous

rough protuberances on the rear surface of the selective layers, except TFC-s-O whose substrate pore size was small. In contrast, all the TFC-n-A membranes formed on aminated substrate showed a smooth rear surface. The protuberances on the rear side of TFC-n-O were considered to be the result of the intrusion of polyamide into the substrate pores.[18, 23, 24] An interesting phenomenon could be noted that, for a series of substrates with different pore sizes, the selective layer formed on the substrate with small pore size (TFC-s-O) had less pronounced protuberances on its rear surface, while substrate with large pore size (TFC-l-O) appeared a more severe polyamide intrusion. This was caused by the large substrate pores disrupting the ideal flat reaction interface during the IP process and shifting the interface toward the interior of the substrate pores.[39] Although the intrusion was helpful in strengthening the mechanical properties, in particularly in the absence of chemical bonding between the substrate and selective layer,[20, 22] it increased the effective thickness of the selective layer and thus introduced additional resistance to water permeation. The limited surface porosity of the substrate made it necessary for water to converge to and pass through these protuberances, rendering the polyamide intrusion as a critical bottleneck for water permeation of TFC membranes (refer to Section 3.3 Separation properties of TFC membranes).

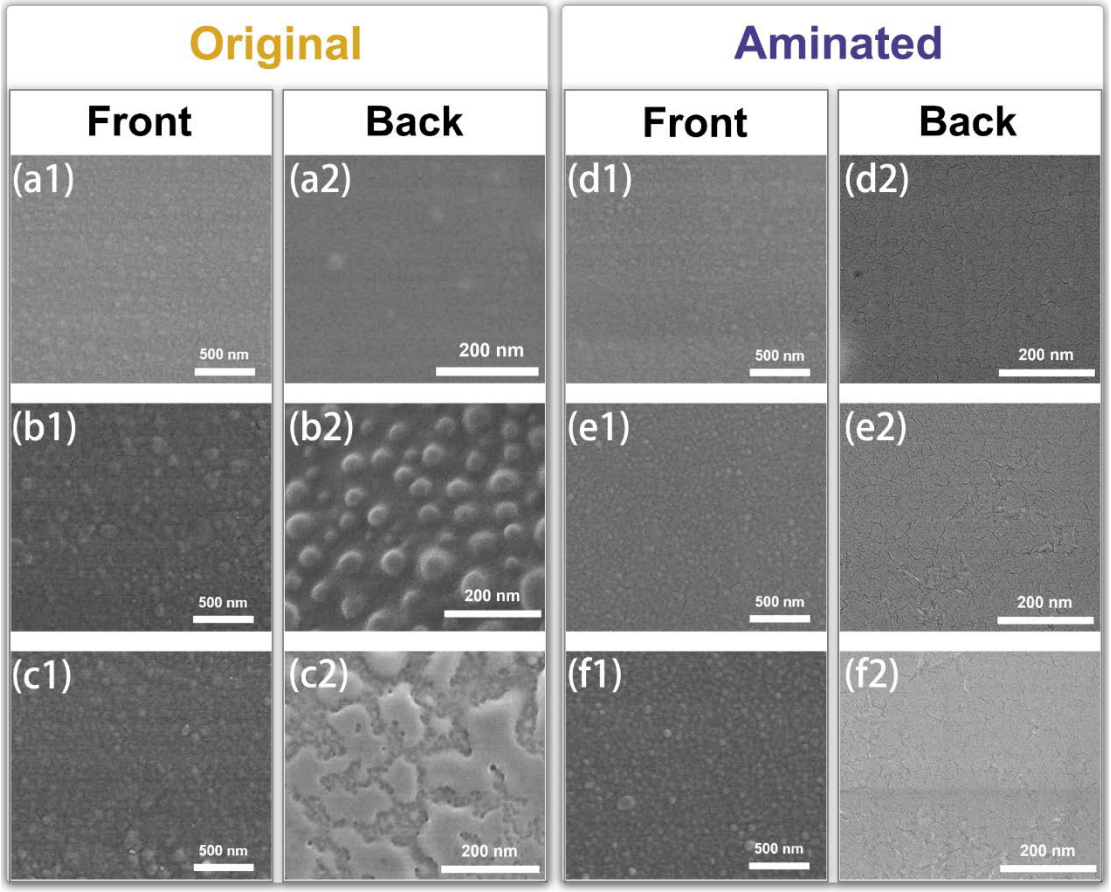

Figure 2. Morphologies of the prepared TFC membranes: (a) TFC-s-O, (b) TFC-m-O, (c) TFC-l-O, (d) TFC-s-A, (e) TFC-m-A, and (f) TFC-l-A. The left panel shows the SEM images of the membrane surfaces, and the right panel in the middle shows the SEM images of the rear side of the selective layers.

To further investigate the structure of TFC-n-O and TFC-n-A, the selective layers were isolated from the TFC membranes and transferred to the silicon wafer by dissolving the substrates, and the thickness of the selective layers were measured by AFM (Figure 3).[40] The average thickness of the selective layers of TFC-s-O, TFC-m-O, TFC-l-O were 38.7 ± 1.1 nm, 41.8 ± 0.5 nm, 44.8 ± 1.2 nm, respectively. While the selective layers of the related TFC-n-A exhibited a smaller average thickness (33.8 ± 0.6 nm, 31.2 ± 0.9 nm, 32.1 ± 0.8 nm for TFC-s-A, TFC-m-A, TFC-l-A, respectively, Table S2). The slightly reduced average thickness of the selective layer could be ascribed to the hindered diffusion of monomers on the aminated substrate, which was also substantiated by the cross-sectional images obtained by TEM (Figure S8).

Compared to TFC-s-O, TFC-m-O and TFC-l-O exhibited increasing maximum thickness due to the presence of the protuberances, indicating that the more severe polyamide intrusion appeared as the pore size of the substrate increased, and thus substantially increased the transport distance and resistance of water molecules inside the selective layer. In contrast, as the pore size of the aminated substrate increased, the maximum thickness of the selective layer of the TFC-n-A prepared by the aminated substrate was maintained at the similar value to its average thickness, confirming the elimination of polyamide intrusion. Notably, the difference in selective layer thickness between TFC-s-O and TFC-s-A was relatively small, indicating that the substrate amination brought a limited enhancement for the substrate with small pore size, due to the absence of polyamide intrusion (Figure 2).

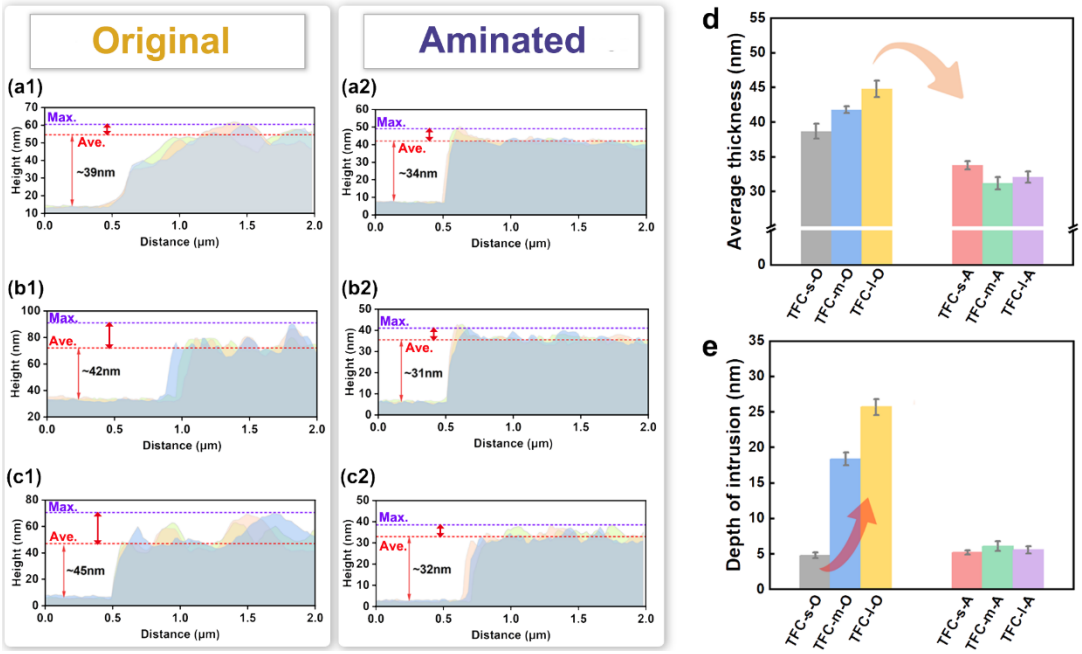

Figure 3. AFM-based profilometry testing of the prepared TFC membranes: (a) TFC-s-O/A, (b) TFC-m-O/A, (c) TFC-l-O/A; (d) Average thickness of the selective layers; (e) Depth of polyamide intrusion of the selective layers.

The results of zeta potential shows that the TFC-n-A had a more negative surface potential compared to the control TFC-n-O, possibly contributing to the separation of charged ions (Figure S9). Table S3 demonstrates the slightly increased O:N ratio of TFC-n-A membranes, further indicating the increased hydrolysis (i.e., reduced degree of cross-linking) of prepared TFC-n-A membranes.[41] The rear side of the selective layers were obtained by dissolving the substrates for further XPS analysis (Figure S10). The obviously increased S content of the corresponding TFC-n-A demonstrated the reactions between the aminated substrates and monomers in the selective layer formation process. Since the reactivity of amino groups (-NH_2) on the aminated substrate surface with acyl chloride groups (-O=C-Cl) in TMC or polyamide oligomers,[24, 42] the aminated substrate could provide a chemical anchorage to bridge the polyamide selective layer with the substrate.

The pore size and pore size distribution of polymer membranes are contemporarily important factors for clarifying the structure-property correlation of membranes, which have a great impact on the membrane separation performance.[43] Figure 4 shows that the TFC-n-A membranes exhibited a higher rejection of uncharged solutes, which indicated their lower MWCO, revealing the enhancement on size sieving effect. Figure

4 further demonstrated that the pore size distribution of TFC-n-A was narrower than that of TFC-n-O, correspondingly. The reduced effective pore size of TFC-n-A was explained by less defect formation in its selective layer, leading to a more uniform pore size distribution (Table S2).[44] This could be the result of a more homogeneous reaction during IP process,[45] thanks to the reactive aminated substrates contained in the TFC-n-A membranes.

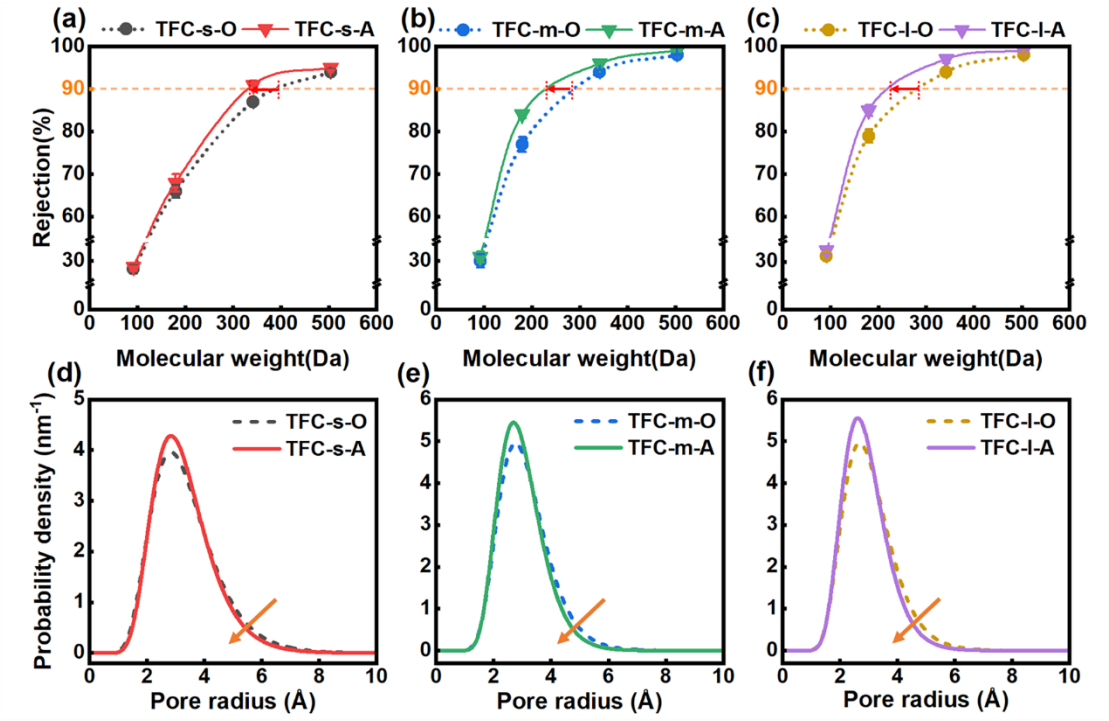

Figure 4. The rejection of neutral molecules including raffinose, sucrose, glucose, and glycerol: (a) TFC-s-O/A, (b) TFC-m-O/A, (c) TFC-l-O/A. The pore size distribution curves of TFC memranes: (d) TFC-s-O/A, (e) TFC-m-O/A, (f) TFC-l-O/A.

3.3 Separation properties of TFC membranes

Figure 5a presents the separation performance of the prepared TFC membranes. TFC-n-O membranes exhibited diminishing water permeance as the pore size of the original substrate increased, even though they had similar average membrane thickness.[46, 47] Interestingly, TFC-l-O prepared on the substrate with relatively large pore size revealed inferior water permeance compared to others. Considering the mitigation of the "funnel effect" by the macroporous substrate, this could be attributed to its exacerbated polyamide intrusion.[47] The water permeance of the TFC-n-A membranes were all improved compared to the control membranes, especially for TFC-l-A with a large pore size substrate, where the water permeance of the membrane was

elevated to 17.5 ± 0.6 $L \cdot m^{-2} \cdot h^{-1} \cdot bar^{-1}$ (Figure 5a). This significant improvement in water permeance occurred after the introduction of amino groups onto the substrate of the TFC-n-A membranes, thanks to the reduced effective thickness of the selective layer and the lack of protuberances (Figure 2, Figure 3). Furthermore, TFC-s-A prepared on the small pore size substrate displayed less improvement in water permeance despite the absence of polyamide intrusion, which confirms the restrictive effect of small pore size substrates on the overall water permeance of TFC membranes.[9, 48]

Compared to TFC-n-O, TFC-n-A exhibited higher rejection of Na_2SO_4 and NaCl (Figure 5a). Typically, TFC-l-A showed the improved NaCl/Na_2SO_4 selectivity, which was obviously higher than other prepared membranes. The enhancement of the size sieving effect and the more negative surface charge promoted the rejection of anions by the TFC-l-A, revealing its optimized separation performance.[5, 49] Figure 5b shows the trade-off relationship between water permeance and salt selectivity for the conventional NF membranes.[50] The TFC membranes prepared in this study (TFC-m-A, TFC-l-A) clearly surpassed the conventional NF membranes by inhibiting polyamide intrusion.

NF membranes with enhanced water permeance and mono/divalent salt selectivity could lead to the dramatic increase in process efficiency.[3, 51] Moreover, membranes with uniform pore size and surface charge distribution show many potential applications, such as the removal of highly toxic trace solutes (e.g., emerging contaminants) from potable water.[52, 53] Figure 5c shows that TFC-l-A exhibited higher rejection of tetracycline (about 98%) compared to the control TFC-l-O. This result can be explained by the enhanced size sieving effect and electrostatic interaction of TFC-l-A, thanks to its lower MWCO and more negative surface potential (Figure S9, Figure 4).

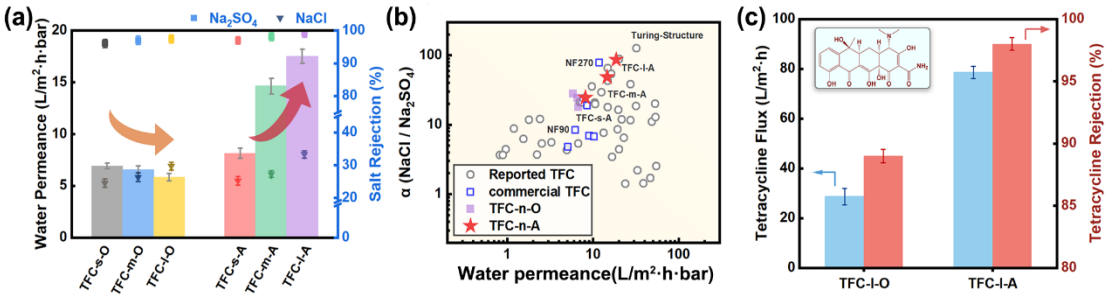

Figure 5. Separation performance of the prepared TFC membranes: (a) water permeance and salts rejection, (b) Na_2SO_4 to NaCl separation factors versus water permeance, (c) Emerging contaminant removal test of TFC membranes with 10 ppm tetracycline as feed solution.

3.4 The strategies to inhibit the polyamide intrusion

To clearly elucidate the mechanism of polyamide intrusion, the relationship between the depth of intrusion and the apparent pore size of substrate was explored by relating the results of this study to the relevant literature (Figure 6a, Table S3).[54] As the pore size of the substrate increased, it inevitably brought about the appearance of polyamide intrusion. The depth of intrusion (λ) was commonly equal to half of the substrate pore size (Figure 6b), and thus the intrusion depth values of TFC membranes prepared by the conventional IP were mostly around this relation line ($\lambda=1/2d_p$). Currently, IP on a particular interlayer was reported as one of the methods to inhibit polyamide intrusion.[23, 25, 55] Indeed, the interlayer was actually more like a smaller pore size and permeation-optimized "substrate", analogous to the small pore size substrate that facilitated the inhibition of intrusion in this study. Furthermore, some researchers inadvertently mitigated the intrusion by optimizing the IP process.[20, 24, 32, 42, 56] The strategy based on the reactive substrate mentioned in this study outperformed other methods of intrusion inhibition, reducing the depth of intrusion to an acceptable value (Figure 6a).

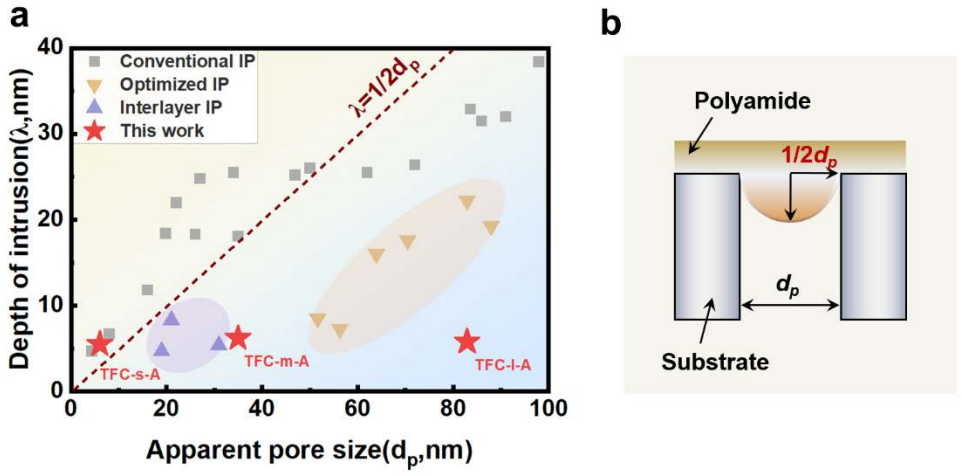

Figure 6. The depth of intrusion versus apparent pore size of substrates. The data collected in these figures include: the TFC membranes prepared in this work, and some reported TFC membranes.[16, 20, 23-25, 32, 38, 39, 42, 54, 56]

To sum up, the first strategy to inhibit polyamide intrusion was to reduce the pore size of the substrate. The aqueous phase solution meniscus might be concave due to the wettability of hydrophilic substrate during the IP process (Figure S6),[17, 18] forcing a portion of the polyamide to form within the substrate pores. The reduction of substrate pore size could enhance the capillary force,[57] mitigating the adverse effect of the

aqueous phase solution meniscus, and thus inhibiting the polyamide intrusion of TFC membranes. Another strategy was to adjust the surface chemical compositions of the substrate according to this study. The introduction of specific reactive groups (including but not limited to amino, hydroxyl) onto the substrate could effectively inhibit the polyamide intrusion without changing the physical properties of the substrate. Although the aqueous phase solution meniscus might remain concave, the reactive groups grafted within the substrate pores could participate in the reaction immediately upon contact with the TMC to form the polyamide in advance, preventing further polyamide growth into the substrate pores.

Although both two strategies were effective in inhibiting polyamide intrusion (Figure 7), the performance of TFC membranes prepared by these strategies could differ entirely (such as TFC-s-A and TFC-l-A). It should be noted that the small pore size substrate normally led to a small substrate porosity during the phase separation preparation process, resulting in the more exacerbated “funnel effect” that adversely affected the water permeance of TFC membranes.[23, 46, 58] Adjusting the surface chemical compositions of the substrate could retain the benefits of the large pore size and high porosity of the substrate, overcoming the limitation of substrates on the overall membrane permeance. In addition, the reactive groups on the aminated substrate surface provided the more uniform distribution of monomers during IP process, breaking the shackle of poor monomer storage capacity of conventional substrates. Meanwhile, these amino groups could contribute to the reduction of selective layer thickness due to their effects on the regulation of monomer diffusion. Therefore, the introduction of amino groups onto the large pore size substrate to inhibit intrusion was the optimal strategy for the design of high-performance TFC membranes.

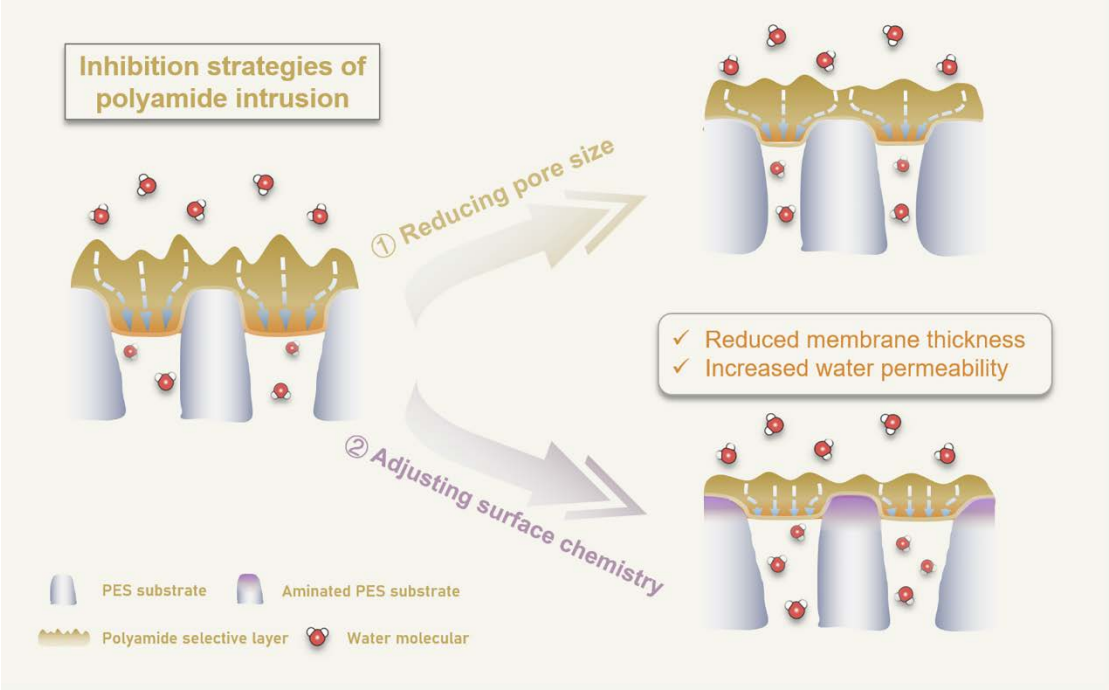

Figure 7. Conceptual model illustrating the mechanism of the inhibition of polyamide intrusion

4. Implication

Our current study demonstrated that optimizing the substrates by reducing the pore sizes, or adjusting the surface chemical compositions via substrate modification could facilitate the inhibition of polyamide intrusion for accurately controlling the structure of selective layers. Particularly, the TFC-l-A prepared under the guidance of the optimal inhibitory strategy exhibited a significant improvement in its water permeance and ionic selectivity. In addition, recent study highlighted the significance of ultra-permeable NF (UPNF) membrane in supporting NF-based water treatment,[51] due to its advantages of enhanced separation efficiency and reduced specific energy consumption (SEC). Tailoring polyamide membranes assisted by intrusion inhibition strategies could be a potential approach to significantly improve membrane permeance, thanks to lower transport distances and resistance. Indeed, the majority of research on substrate optimization (or interlayer) was still at the theoretical stage,[59, 60] yet few of them have been applied in commercial applications. Our inhibitory strategies were prospectively feasible in practical production, which made it possible to manufacture the UPNF membranes with structurally optimized selective layers in one step production.

We further found that TFC-l-A with inhibited polyamide intrusion exhibited higher rejection of emerging contaminant, due to the normalized pores and reduced defects in

selective layer.[36, 52] Since the inhibition of intrusion theoretically affected only the permeance of the selective layer, this might be caused by the aminated substrate. Besides the reactivity, the amino groups could promote the formation of a more homogeneous reaction interface and thus reduced defects in the selective layer. Interestingly, the reduction in the effective thickness of the selective layer implied a positive contribution to membrane permeance by diffusion regulation of the aminated substrate. However, the underlying mechanisms of chemical groups on the substrate surface affecting the monomer diffusion remain unclear. Future studies need to crystallize this diffusion-regulated effect during IP process. The excellent emerging contaminant removal combined with the simultaneously improved membrane permeance and selectivity, confers polyamide intrusion inhibition a strong potential for the state-of-the-art membrane design.

ASSOCIATED CONTENT

Supporting Information: Surface amination of substrates (Figure S1); The experimental parameters of PIP diffusion (Figure S2); Standard curve of tetracycline in solution (Figure S3); The surface morphologies of substrates (Figure S4); Morphologies of substrates (Figure S5); The water contact angle of prepared substrates (Figure S6); Morphologies of the TFC membranes (Figure S7); Cross-sectional structure of TFC membranes (Figure S8); Zeta potential curves of TFC membranes (Figure S9); XPS spectra of the rear side of the selective layers (Figure S10); Anti-fouling performance of TFC membranes (Figure S11); Long-term stability of TFC-l-A (Figure S12).

AUTHOR INFORMATION

Corresponding Authors

Zhikan Yao - MOE Engineering Research Center of Membrane and Water Treatment Technology, College of Chemical and Biological Engineering, Zhejiang University, Hangzhou, 310027, P. R. China; Shanxi-Zheda Institute of Advanced Materials and Chemical Engineering, Taiyuan, 030000, P.R. China; orcid.org/0000-0002-3398-3029

E-mail: yaozhikan@zju.edu.cn

Authors

Yukun Qian - MOE Engineering Research Center of Membrane and Water Treatment Technology, College of Chemical and Biological Engineering, Zhejiang University, Hangzhou, 310027, P. R. China

Haozheng Li - MOE Engineering Research Center of Membrane and Water Treatment Technology, College of Chemical and Biological Engineering, Zhejiang University, Hangzhou, 310027, P. R. China

Jiancong Lu – Ocean College, Zhejiang University, Zhoushan, 316021, P. R. China

Dan Lu - MOE Engineering Research Center of Membrane and Water Treatment Technology, College of Chemical and Biological Engineering, Zhejiang University, Hangzhou, 310027, P. R. China

Hongyu Jin - MOE Engineering Research Center of Membrane and Water Treatment Technology, College of Chemical and Biological Engineering, Zhejiang University, Hangzhou, 310027, P. R. China

Zhiyi Xia - MOE Engineering Research Center of Membrane and Water Treatment Technology, College of Chemical and Biological Engineering, Zhejiang University, Hangzhou, 310027, P. R. China

Jing Wang - MOE Engineering Research Center of Membrane and Water Treatment Technology, College of Chemical and Biological Engineering, Zhejiang University, Hangzhou, 310027, P. R. China; Ningbo Research Institute, Zhejiang University, Ningbo, 315100, P. R. China

Lin Zhang - MOE Engineering Research Center of Membrane and Water Treatment Technology, College of Chemical and Biological Engineering, Zhejiang University, Hangzhou, 310027, P. R. China; Institute of Zhejiang University-Quzhou, 78 Jiuhua Boulevard North, Quzhou, 324000, P. R. China; Ningbo Research Institute, Zhejiang University, Ningbo, 315100, P. R. China; orcid.org/0000-0002-1337-2538

Chuyang Y. Tang - Department of Civil Engineering, The University of Hong Kong, Hong Kong SAR 999077, P. R. China; China; orcid.org/0000-0002-7932-6462

Notes

The authors declare no competing financial interest.

ACKNOWLEDGMENTS

The work described in this paper was supported by the "Pioneer" and "Leading Goose" R&D Program of Zhejiang (2023C03150), the National Natural Science Foundation of China (21908192, U21A20302, 22108247), Ecological Civilization Project of Zhejiang University, and Shanxi-Zheda Institute of Advanced Materials and Chemical Engineering (2022SZ-TD002).

We acknowledge the help on zeta potential analysis by Mr. Sanchuan Yu, TOC analysis by Dr. Ying Li, and XPS spectra analysis by Ms. Yangfan Lu at the School of Materials Science and Engineering at Zhejiang University. We thank Mr. Nianhang Rong, and Ms. Xiaomin Zhang for their assistance in SEM and TEM analysis at the Analysis Center of Agrobiology and Environmental Sciences at Zhejiang University. We also appreciate Ms. Sudan Shen, and Ms. Jing He for their assistance in the performance TEM, and AFM analysis at the State Key Laboratory of Chemical Engineering at Zhejiang University.

REFERENCES

1. Tang, C. Y.; Yang, Z.; Guo, H.; Wen, J. J.; Nghiem, L. D.; Cornelissen, E., Potable Water Reuse through Advanced Membrane Technology. *Environ. Sci. Technol.* **2018,** *52*, (18), 10215-10223.

2. Xu, S.; Song, J.; Bi, Q.; Chen, Q.; Zhang, W.-M.; Qian, Z.; Zhang, L.; Xu, S.; Tang, N.; He, T., Extraction of lithium from Chinese salt-lake brines by membranes: Design and practice. *J. Membr. Sci.* **2021,** *635*, 119441.

3. Guo, H.; Li, X.; Yang, W.; Yao, Z.; Mei, Y.; Peng, L. E.; Yang, Z.; Shao, S.; Tang, C. Y., Nanofiltration for drinking water treatment: a review. *Front. Chem. Sci. Eng.* **2022,** *16*, (5), 681-698.

4. Werber, J. R.; Osuji, C. O.; Elimelech, M., Materials for next-generation desalination and water purification membranes. *Nat. Rev. Mater.* **2016,** *1*, (5), 16018.

5. Lu, D.; Yao, Z.; Jiao, L.; Waheed, M.; Sun, Z.; Zhang, L., Separation mechanism, selectivity enhancement strategies and advanced materials for mono-/multivalent ion-selective nanofiltration membrane. *Adv. Membr.* **2022,** *2*, 100032.

6. Zhao, Y.; Tong, T.; Wang, X.; Lin, S.; Reid, E. M.; Chen, Y., Differentiating Solutes with Precise Nanofiltration for Next Generation Environmental Separations: A Review. *Environ. Sci. Technol.* **2021,** *55*, (3), 1359-1376.

7. Lu, X.; Elimelech, M., Fabrication of desalination membranes by interfacial polymerization: history, current efforts, and future directions. *Chem. Soc. Rev.* **2021,** *50*, (11), 6290-6307.

8. Wang, K.; Wang, X.; Januszewski, B.; Liu, Y.; Li, D.; Fu, R.; Elimelech, M.; Huang, X., Tailored design of nanofiltration membranes for water treatment based on synthesis-property-performance relationships. *Chem. Soc. Rev.* **2022,** *51*, (2), 672-719.

9. Karan, S.; Jiang, Z.; Livingston, A. G., Sub-10 nm polyamide nanofilms with ultrafast solvent transport for molecular separation. *Science* **2015,** *348*, (6241), 1347-1351.

10. Freger, V.; Ramon, G. Z., Polyamide desalination membranes: Formation, structure, and properties. *Prog. Polym. Sci.* **2021,** *122*, 101451.

11. Han, S.; Zhu, J.; Uliana, A. A.; Li, D.; Zhang, Y.; Zhang, L.; Wang, Y.; He, T.; Elimelech, M., Microporous organic nanotube assisted design of high performance nanofiltration membranes. *Nat. Commun.* **2022,** *13*, (1), 7954.

12. Tan, Z.; Chen, S.; Peng, X.; Zhang, L.; Gao, C., Polyamide membranes with nanoscale Turing structures for water purification. *Science* **2018,** *360*, (6388), 518-521.

13. Lu, D.; Ma, T.; Lin, S.; Zhou, Z.; Li, G.; An, Q.; Yao, Z.; Sun, Q.; Sun, Z.; Zhang, L., Constructing a selective blocked-nanolayer on nanofiltration membrane via surface-charge inversion for promoting Li+ permselectivity over Mg2+. *J. Membr. Sci.* **2021,** *635*, 119504.

14. Feng, X.; Liu, D.; Ye, H.; Peng, D.; Wang, J.; Han, S.; Zhang, Y., High-flux polyamide membrane with improved chlorine resistance for efficient dye/salt separation based on a new N-rich amine monomer. *Sep. Purif. Technol.* **2021,** *278*, 120987.

15. Shao, S.; Zeng, F.; Long, L.; Zhu, X.; Peng, L. E.; Wang, F.; Yang, Z.; Tang, C. Y., Nanofiltration Membranes with Crumpled Polyamide Films: A Critical Review on Mechanisms, Performances, and Environmental Applications. *Environ. Sci. Technol.*

2022, *56*, (18), 12811-12827.

16. Peng, L. E.; Yang, Z.; Long, L.; Zhou, S.; Guo, H.; Tang, C. Y., A critical review on porous substrates of TFC polyamide membranes: Mechanisms, membrane performances, and future perspectives. *J. Membr. Sci.* **2022,** *641*, 119871.

17. Dai, R.; Yang, Z.; Qiu, Z.; Long, L.; Tang, C. Y.; Wang, Z., Distinct impact of substrate hydrophilicity on performance and structure of TFC NF and RO polyamide membranes. *J. Membr. Sci.* **2022,** *662*, 120966.

18. Ghosh, A. K.; Hoek, E. M. V., Impacts of support membrane structure and chemistry on polyamide–polysulfone interfacial composite membranes. *J. Membr. Sci.* **2009,** *336*, (1-2), 140-148.

19. Jimenez-Solomon, M. F.; Gorgojo, P.; Munoz-Ibanez, M.; Livingston, A. G., Beneath the surface: Influence of supports on thin film composite membranes by interfacial polymerization for organic solvent nanofiltration. *J. Membr. Sci.* **2013,** *448*, 102-113.

20. Lu, X.; Nejati, S.; Choo, Y.; Osuji, C. O.; Ma, J.; Elimelech, M., Elements Provide a Clue: Nanoscale Characterization of Thin-Film Composite Polyamide Membranes. *ACS Appl. Mater. Interfaces* **2015,** *7*, (31), 16917-22.

21. Huang, L.; McCutcheon, J. R., Impact of support layer pore size on performance of thin film composite membranes for forward osmosis. *J. Membr. Sci.* **2015,** *483*, 25-33.

22. Luo, F.; Wang, J.; Yao, Z.; Zhang, L.; Chen, H., Polydopamine nanoparticles modified nanofiber supported thin film composite membrane with enhanced adhesion strength for forward osmosis. *J. Membr. Sci.* **2021,** *618*, 118673.

23. Yang, Z.; Zhou, Z. W.; Guo, H.; Yao, Z.; Ma, X. H.; Song, X.; Feng, S. P.; Tang, C. Y., Tannic Acid/Fe(3+) Nanoscaffold for Interfacial Polymerization: Toward Enhanced Nanofiltration Performance. *Environ. Sci. Technol.* **2018,** *52*, (16), 9341-9349.

24. Ji, X.; Li, G.; Chen, G.; Qian, Y.; Jin, H.; Yao, Z.; Zhang, L., Aminated substrate based thin film composite nanofiltration membrane with high separation performance by chemically inhibiting the intrusion of polyamide. *Desalination* **2022,** *532*, 115724.

25. Zhou, Z.; Hu, Y.; Boo, C.; Liu, Z.; Li, J.; Deng, L.; An, X., High-Performance Thin-

Film Composite Membrane with an Ultrathin Spray-Coated Carbon Nanotube Interlayer. *Environ. Sci. Technol. Lett.* **2018,** *5*, (5), 243-248.

26. Yang, Z.; Wu, Y.; Wang, J.; Cao, B.; Tang, C. Y., In Situ Reduction of Silver by Polydopamine: A Novel Antimicrobial Modification of a Thin-Film Composite Polyamide Membrane. *Environ. Sci. Technol.* **2016,** *50*, (17), 9543-50.

27. Culp, T. E.; Shen, Y.-x.; Geitner, M.; Paul, M.; Roy, A.; Behr, M. J.; Rosenberg, S.; Gu, J.; Kumar, M.; Gomez, E. D., Electron tomography reveals details of the internal microstructure of desalination membranes. *Proc. Natl. Acad. Sci.* **2018,** *115*, (35), 8694-8699.

28. Singh, S.; Khulbe, K. C.; Matsuura, T.; Ramamurthy, P., Membrane characterization by solute transport and atomic force microscopy. *J. Membr. Sci.* **1998,** *142*, (1), 111-127.

29. Liang, Y.; Zhu, Y.; Liu, C.; Lee, K. R.; Hung, W. S.; Wang, Z.; Li, Y.; Elimelech, M.; Jin, J.; Lin, S., Polyamide nanofiltration membrane with highly uniform sub-nanometre pores for sub-1 A precision separation. *Nat. Commun.* **2020,** *11*, (1), 2015.

30. Ding, J.; Wu, H.; Wu, P., Multirole Regulations of Interfacial Polymerization Using Poly(acrylic acid) for Nanofiltration Membrane Development. *ACS Appl. Mater. Interfaces* **2021,** 13, (44), 53120–53130.

31. Wang, Z.; Liang, S.; Jin, Y.; Zhao, L.; Hu, L., Controlling structure and properties of polyamide nanofilms by varying amines diffusivity in organic phase. *J. Membr. Sci.* **2019,** *574*, 1-9.

32. Yao, Z.; Guo, H.; Yang, Z.; Qing, W.; Tang, C. Y., Preparation of nanocavity-contained thin film composite nanofiltration membranes with enhanced permeability and divalent to monovalent ion selectivity. *Desalination* **2018,** *445*, 115-122.

33. Wang, R.; Zhang, J.; Tang, C. Y.; Lin, S., Understanding Selectivity in Solute-Solute Separation: Definitions, Measurements, and Comparability. *Environ. Sci. Technol.* **2022,** *56*, (4), 2605-2616.

34. Xu, S.; He, R.; Zhao, S.; Shon, H. K.; He, T., Is conductivity measurement or inductively coupled plasma-atomic emission spectrometry reliable to define rejection of different ions? *Desalination* **2022,** *543*, 116097.

35. Geise, G. M., Experimental characterization of polymeric membranes for selective ion transport. *Curr. Opin. Chem. Eng.* **2020,** *28*, 36-42.

36. Guo, H.; Deng, Y.; Tao, Z.; Yao, Z.; Wang, J.; Lin, C.; Zhang, T.; Zhu, B.; Tang, C. Y., Does Hydrophilic Polydopamine Coating Enhance Membrane Rejection of Hydrophobic Endocrine-Disrupting Compounds? *Environ. Sci. Technol. Lett.* **2016,** *3*, (9), 332-338.

37. Hoseinpour, V.; Ghaee, A.; Vatanpour, V.; Ghaemi, N., Surface modification of PES membrane via aminolysis and immobilization of carboxymethylcellulose and sulphated carboxymethylcellulose for hemodialysis. *Carbohydr. Polym.* **2018,** *188*, 37-47.

38. Yang, X.; Du, Y.; Zhang, X.; He, A.; Xu, Z. K., Nanofiltration Membrane with a Mussel-Inspired Interlayer for Improved Permeation Performance. *Langmuir* **2017,** *33*, (9), 2318-2324.

39. Peng, L. E.; Yao, Z.; Yang, Z.; Guo, H.; Tang, C. Y., Dissecting the Role of Substrate on the Morphology and Separation Properties of Thin Film Composite Polyamide Membranes: Seeing Is Believing. *Environ. Sci. Technol.* **2020,** *54*, (11), 6978-6986.

40. Lin, L.; Feng, C.; Lopez, R.; Coronell, O., Identifying facile and accurate methods to measure the thickness of the active layers of thin-film composite membranes – A comparison of seven characterization techniques. *J. Membr. Sci.* **2016,** *498*, 167-179.

41. Tang, C. Y.; Kwon, Y.-N.; Leckie, J. O., Effect of membrane chemistry and coating layer on physiochemical properties of thin film composite polyamide RO and NF membranes: I. FTIR and XPS characterization of polyamide and coating layer chemistry. *Desalination* **2009,** *242*, (1), 149-167.

42. Yao, Z.; Guo, H.; Yang, Z.; Lin, C.; Zhu, B.; Dong, Y.; Tang, C. Y., Reactable substrate participating interfacial polymerization for thin film composite membranes with enhanced salt rejection performance. *Desalination* **2018,** *436*, 1-7.

43. Gin, D. L.; Noble, R. D., Designing the Next Generation of Chemical Separation Membranes. *Science* **2011,** *332*, (6030), 674-676.

44. Yang, Z.; Sun, P. F.; Li, X.; Gan, B.; Wang, L.; Song, X.; Park, H. D.; Tang, C. Y., A Critical Review on Thin-Film Nanocomposite Membranes with Interlayered

Structure: Mechanisms, Recent Developments, and Environmental Applications. *Environ. Sci. Technol.* **2020,** *54*, (24), 15563-15583.

45. Liu, L.; Chen, X.; Feng, S.; Wan, Y.; Luo, J., Enhancing the Antifouling Ability of a Polyamide Nanofiltration Membrane by Narrowing the Pore Size Distribution via One-Step Multiple Interfacial Polymerization. *ACS Appl. Mater. Interfaces* **2022,** *14*, (31), 36132-36142.

46. Li, X.; Li, Q.; Fang, W.; Wang, R.; Krantz, W. B., Effects of the support on the characteristics and permselectivity of thin film composite membranes. *J. Membr. Sci.* **2019,** *580*, 12-23.

47. Wang, F.; Yang, Z.; Tang, C. Y., Modeling Water Transport in Interlayered Thin-Film Nanocomposite Membranes: Gutter Effect vs Funnel Effect. *ACS ES&T Engg.* **2022,** 2, (11), 2023-2033.

48. Jiang, Z.; Karan, S.; Livingston, A. G., Water Transport through Ultrathin Polyamide Nanofilms Used for Reverse Osmosis. *Adv. Mater.* **2018,** *30*, (15), e1705973.

49. Zhai, X.; Wang, Y. L.; Dai, R.; Li, X.; Wang, Z., Roles of Anion-Cation Coupling Transport and Dehydration-Induced Ion-Membrane Interaction in Precise Separation of Ions by Nanofiltration Membranes. *Environ. Sci. Technol.* **2022,** *56*, (19), 14069-14079.

50. Yang, Z.; Guo, H.; Tang, C. Y., The upper bound of thin-film composite (TFC) polyamide membranes for desalination. *J. Membr. Sci.* **2019,** *590*, 117297.

51. Yang, Z.; Wu, C.; Tang, C. Y., Making waves: Why do we need ultra-permeable nanofiltration membranes for water treatment? *Water Res. X* **2023,** *19*, 100172.

52. Gao, Y.; Zhao, Y.; Wang, X. M.; Tang, C.; Huang, X., Modulating the Asymmetry of the Active Layer in Pursuit of Nanofiltration Selectivity via Differentiating Interfacial Reactions of Piperazine. *Environ. Sci. Technol.* **2022,** *56*, (19), 14038-14047.

53. Liang, Y.; Lin, S., Mechanism of Permselectivity Enhancement in Polyelectrolyte-Dense Nanofiltration Membranes via Surfactant-Assembly Intercalation. *Environ. Sci. Technol.* **2021,** *55*, (1), 738-748.

54. Song, X.; Gan, B.; Qi, S.; Guo, H.; Tang, C. Y.; Zhou, Y.; Gao, C., Intrinsic Nanoscale Structure of Thin Film Composite Polyamide Membranes: Connectivity, Defects, and Structure-Property Correlation. *Environ. Sci. Technol.* **2020,** *54*, (6), 3559-

3569.

55. Yang, Z.; Wang, F.; Guo, H.; Peng, L. E.; Ma, X. H.; Song, X. X.; Wang, Z.; Tang, C. Y., Mechanistic Insights into the Role of Polydopamine Interlayer toward Improved Separation Performance of Polyamide Nanofiltration Membranes. *Environ. Sci. Technol.* **2020,** *54*, (18), 11611-11621.

56. Park, S.-J.; Ahn, W.-G.; Choi, W.; Park, S.-H.; Lee, J. S.; Jung, H. W.; Lee, J.-H., A facile and scalable fabrication method for thin film composite reverse osmosis membranes: dual-layer slot coating. *J. Mater. Chem. A* **2017,** *5*, (14), 6648-6655.

57. Jiang, C.; Tian, L.; Zhai, Z.; Shen, Y.; Dong, W.; He, M.; Hou, Y.; Niu, Q. J., Thin-film composite membranes with aqueous template-induced surface nanostructures for enhanced nanofiltration. *J. Membr. Sci.* **2019,** *589*, 117244.

58. Ramon, G. Z.; Wong, M. C. Y.; Hoek, E. M. V., Transport through composite membrane, part 1: Is there an optimal support membrane?. *J. Membr. Sci.* **2012,** *415-416*, 298-305.

59. Beuscher, U.; Kappert, E. J.; Wijmans, J. G., Membrane research beyond materials science. *J. Membr. Sci.* **2022,** *643*, 119902.

60. Zhou, H.; Dai, R.; Wang, T.; Wang, Z., Enhancing Stability of Tannic Acid-Fe(III) Nanofiltration Membrane for Water Treatment: Intercoordination by Metal-Organic Framework. *Environ. Sci. Technol.* **2022,** *56*, (23), 17266-17277.

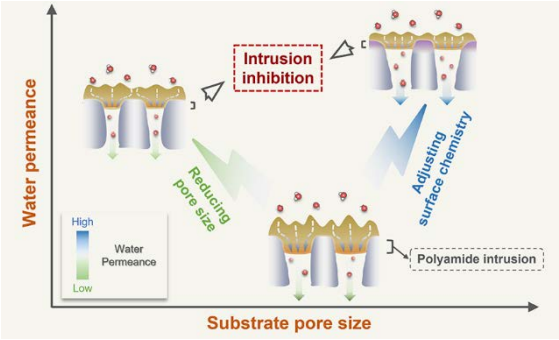

Abstract Graphic